



Showcasing research from Professors Leman's and Krishnamurthy's laboratory, Department of Chemistry, The Scripps Research Institute, California, USA.

One-pot chemical pyro- and tri-phosphorylation of peptides by using diamidophosphate in water

Pyrophosphopeptides are produced in good yields from diamidophosphate mediated phosphorylation of phosphopeptides followed by hydrolysis of the resulting amidopyrophosphate. The overall reaction proceeds efficiently in water-ice medium without the need for protecting groups. The simplicity of this process enables a repetitive phosphorylation-hydrolysis sequence of reactions in a single pot that produces triphosphopeptides efficiently. The potential for continual reiteration of this sequence of reactions suggests that it can become a practical synthetic tool for protein polyphosphorylation.

As featured in:



See Huacan Lin, Luke J. Leman, Ramanarayanan Krishnamurthy, *Chem. Sci.*, 2022, 13, 13741.

Cite this: *Chem. Sci.*, 2022, 13, 13741

All publication charges for this article have been paid for by the Royal Society of Chemistry

Received 26th July 2022  
Accepted 30th October 2022

DOI: 10.1039/d2sc04160j

rsc.li/chemical-science

# One-pot chemical pyro- and tri-phosphorylation of peptides by using diamidophosphate in water†

Huacan Lin,<sup>1</sup> Luke J. Leman<sup>1</sup> and Ramanarayanan Krishnamurthy<sup>1</sup>

Protein (pyro)phosphorylation is emerging as a post-translational modification (PTM) in signalling pathways involved in many cellular processes. However, access to synthetic pyrophosphopeptides that can serve as tools for understanding protein pyrophosphorylation is quite limited. Herein, we report a chemical phosphorylation method that enables the synthesis of pyrophosphopeptides in aqueous medium without the need for protecting groups. The strategy employs diamidophosphate (DAP) in a one-pot sequential phosphorylation-hydrolysis of mono-phosphorylated peptide precursors. This operationally simple method exploits the intrinsic nucleophilicity of a phosphate moiety installed on serine, threonine or tyrosine residues in complex peptides with excellent chemoselectivity and good yields under mild conditions. We demonstrate the installation of the pyrophosphate group within a wide range of model peptides and showcase the potential of this methodology by selectively pyrophosphorylating the highly functionalized Nopp140 peptide fragment. The potential to produce higher (poly)phosphorylated peptides was demonstrated as a proof-of-principle experiment where we synthesized the triphosphorylated peptides using this one-pot strategy.

## Introduction

Post-translational modifications (PTMs) play significant roles in modulating protein function and activity.<sup>1</sup> Among a broad range of PTMs,<sup>2–6</sup> protein phosphorylation arguably is the most widely studied PTM and plays a crucial role in regulating many other cellular processes. Since its discovery in 1959,<sup>7</sup> phosphorylation has been closely linked with many cellular functions in the cell cycle,<sup>8</sup> apoptosis,<sup>9</sup> differentiation<sup>10</sup> and others. Various techniques for enrichment of phosphorylated proteins as well as their identification and quantitation are accessible today for the analysis of phosphorylation.<sup>11</sup> In contrast to protein phosphorylation, protein pyrophosphorylation is a poorly characterized PTM. It is known to be mediated by a group of second messengers termed inositol pyrophosphates (PP-InsPs)<sup>12</sup> which are capable of transferring the beta-phosphoryl group from 5PP-InsP<sub>5</sub> in the presence of Mg<sup>2+</sup> to a phosphorylated serine residue in protein substrates to generate a pyrophosphorylated protein (Fig. 1a).<sup>13,14</sup> Some significant advancements have been made in understanding the important roles that inositol pyrophosphates play in various pathways.<sup>15–18</sup> Even so, the biological functions of protein pyrophosphorylation remain largely unknown due to the

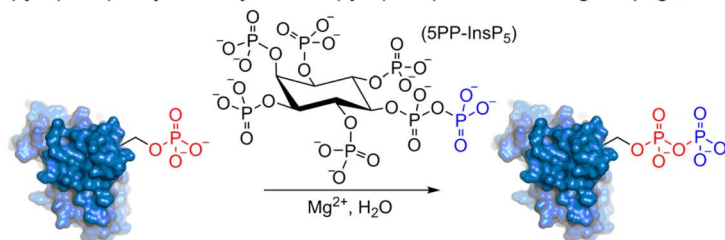
difficulty in identifying pyrophosphorylated proteins in complex cellular contexts and the few efficient methodologies for chemically synthesizing pyrophosphorylated peptides and proteins *in vitro*. Thus, there is a need to develop new methods and expand the toolbox for accessible peptide and protein pyrophosphorylation.

In 2014, Fiedler and co-workers reported a synthetic methodology to access pyrophosphorylated peptides and proteins from phosphorylated precursors (Fig. 1b).<sup>19,20</sup> This protocol involves pyrophosphorylation of a phosphoserine residue by using a benzyl phosphorimidazole reagent in water/dimethylacetamide co-solvent as the first step, followed by hydrogenolysis of the isolated benzyl-protected intermediates in water/dimethylformamide co-solvent to provide the pyrophosphopeptides. This protocol also proceeded in water but with slower reaction kinetics. Surprisingly, there are no other methods available that allow easy access to pyrophosphorylated peptides, despite the considerable number of synthetic approaches for polyphosphorylation of small molecules such as nucleosides.<sup>21–24</sup> Here, we present a simple one-pot chemical strategy for the facile synthesis of pyrophosphopeptides. Our approach starts from a peptide precursor bearing a phosphorylated Ser, Thr or Tyr residue, which site-selectively reacts with diamidophosphate (DAP) in water to generate an amidopyrophosphorylated intermediate, followed by nitrous acid-induced hydrolysis to afford the expected pyrophosphopeptide (Fig. 1c). Distinct from the existing method, our approach does not require protecting/

Department of Chemistry, The Scripps Research Institute, La Jolla, California 92037, USA. E-mail: hulin@scripps.edu; lleman@scripps.edu; rkrishna@scripps.edu

† Electronic supplementary information (ESI) available: Experimental procedures, synthetic schemes, HPLC traces and MS spectra. See DOI: <https://doi.org/10.1039/d2sc04160j>



(a) Protein pyrophosphorylation by inositol pyrophosphate messengers (e.g., 5PP-InsP<sub>5</sub>)

(b) Peptide pyrophosphorylation by using phosphorimidazolide and subsequent hydrogenolysis



(c) This work:

Peptide pyrophosphorylation by using diamidophosphate and subsequent hydrolysis



Chemoselective ✓ Simple operation ✓ High conversion ✓  
 One-pot in aqueous media ✓ Wide compatibility with canonical amino acids ✓

**Fig. 1** Site-selective peptide pyrophosphorylation via a one-pot sequential amidophosphorylation-hydrolysis methodology. (a) Inositol pyrophosphate messenger-mediated protein pyrophosphorylation in the presence of magnesium. (b) Chemical pyrophosphorylation of peptides using phosphorimidazolide reagents.<sup>29</sup> (c) Diamidophosphate-mediated site-selective pyrophosphorylation of peptides. The use of diamidophosphate in aqueous medium, presented in this work, offers several advantages. Circles represent amino acids; DMA, dimethylacetamide; DMF, dimethylformamide.

deprotecting group chemistry, or isolation of peptide intermediates. Furthermore, this higher yielding one-pot transformation displays excellent selectivity for phosphate moieties over the other nucleophilic peptide side chains, and wide applicability for accessing various synthetic and native pyrophosphopeptides.

## Results and discussion

Previous work from our group showed that DAP, which was prepared *via* saponification of phenyl phosphorodiamidate, is a versatile phosphorylating agent.<sup>25</sup> Particularly, DAP reacted with 5'-nucleoside monophosphates (5'-NMPs) and 5'-nucleoside diphosphates (5'-NDPs) to generate the corresponding 5'-amidodiphosphate and 5'-amidotriphosphate derivatives, respectively, and converted 2',3'-ribonucleotides to the corresponding 2',3'-cyclic-phosphates.<sup>26</sup> Recently, we showed that DAP enables the conversion of 5'-NMPs and 5'-oligonucleotide monophosphates into the corresponding nucleoside triphosphates (5'-NTPs) and 5'-oligonucleotide triphosphates *via* amidophosphates in a one-pot amidophosphorylation-hydrolysis setting in water.<sup>27</sup> Inspired by these observations, we reasoned that phosphopeptides might also undergo a similar amidophosphorylation-hydrolysis to afford the corresponding pyrophosphopeptides in one-pot,<sup>28,29</sup> considering the plausible

reactive groups in the side chains (e.g., lysine, aspartate, glutamate, cysteine, *etc.*).

To test this hypothesis, 1 mM peptide **1** (Ac-WN**S**ANG-CONH<sub>2</sub>, phosphoserine indicated in bold and red, prepared by the incorporation of commercially available Fmoc-*O*-benzyl-phosphoserine, ESI Fig. S2†),<sup>30</sup> was treated with an excess of DAP (30 equiv.), MgCl<sub>2</sub> (10 equiv.) and imidazole (10 equiv.) at pH 5.5 in water at room temperature, 45 °C or −20 °C (in a freezer). The formation of the amidopyrophosphopeptide **19** in the crude reaction mixture was monitored by reverse-phase high-performance liquid chromatography (HPLC) and mass spectrometry (MS). Imidazole acts as a catalyst to increase the efficiency of the amidophosphorylation reaction of the phosphopeptide by forming the amidophosphorimidazolide intermediate *in situ*.<sup>26</sup> Encouragingly, we observed almost full consumption of the starting peptide **1** after 48 hours to produce amidopyrophosphopeptide **19** with 91% conversion at −20 °C as indicated by HPLC, while significantly lower conversions of 22% and 20% were obtained at room temperature and 45 °C, respectively (ESI Fig. S23–S25†). The excellent conversion at −20 °C was consistent with our previous results indicating that the eutectic concentrating environment of water-ice enabled efficient formation of ribonucleoside 2',3'-cyclophosphate from the corresponding ribonucleoside 3'-monophosphates (3'-NMPs) in the presence



of DAP, MgCl<sub>2</sub> and imidazole.<sup>31</sup> We attribute this significantly higher yield observed at  $-20\text{ }^{\circ}\text{C}$  to (a) the freeze concentration effect<sup>32</sup> in co-existing water-ice phases, an effect seen in other contexts<sup>27,33</sup> and (b) a much slower hydrolytic degradation of DAP (when compared to room temperature and  $45\text{ }^{\circ}\text{C}$ ), which allows the DAP to be available for the phosphorylation reaction over a longer period of time (see ESI Fig. S26–S31† for details). Through further investigations, we found that decreasing the amounts of DAP (5 equiv.), MgCl<sub>2</sub> (2 equiv.) and imidazole (2 equiv.) still produced **19** with 86% conversion (Table 1, entry 1, and ESI Fig. S34†). Thus, we adopted these conditions for future amidophosphorylation reactions.

For the hydrolysis step, 5 equiv. of sodium nitrite were added to the crude **19** in the same pot and the pH was adjusted to 3.0 and left at  $-20\text{ }^{\circ}\text{C}$ . Monitoring by HPLC showed complete conversion of amidopyrophosphopeptide **19** into pyrophosphopeptide **35** after an additional 20 hours at  $-20\text{ }^{\circ}\text{C}$ . This resulted in overall 85% conversion over two steps starting from **1**, as confirmed by LC-MS (Table 1, entry 1 and ESI Fig. S35†), suggesting that the nitrous acid-induced hydrolysis of the amidopyrophosphate group in **19** was almost quantitative. Having established appropriate conditions, we sought to evaluate the functional group tolerance by incorporating other amino acids with nucleophiles in their side chains. Peptide **2** (Ac-WKNA**S**ANG-CONH<sub>2</sub>, and ESI Fig. S3†) bearing a reactive lysine proceeded efficiently and produced the expected amidopyrophosphopeptide **20** with near quantitative conversion at 96% as confirmed by LC-MS (Table 1, entry 2 and ESI Fig. S36†). Treatment of crude **20** with NaNO<sub>2</sub> at pH 3.0 produced pyrophosphopeptide **36** as the desired product with 95% conversion over two steps (Table 1, entry 2 and ESI Fig. S37†).

As a representative example for investigating the effect of the position of the phosphate group on the efficiency and selectivity, we chose peptide **3** (Ac-**S**WHNAANG-CONH<sub>2</sub>, and ESI Fig. S4†), which has a phosphoserine at the N-terminal residue with a neighboring histidine unit (Table 1, entry 3). Almost full conversion to the amidopyrophosphopeptide **21** (97%) and pyrophosphopeptide **37** (96% over two steps from the starting peptide **3**) were observed under the conditions as indicated by HPLC analysis (Fig. 2). No other by-products were detectable during the formation of **21** and **37**. Although the retention times for **21** and **37** were close, the 1-unit difference in  $[\text{M} - \text{H}]^{-}$  and 0.5-unit difference in  $[\text{M} - 2\text{H}]^{2-}$  between the amidopyrophosphopeptide ion and pyrophosphopeptide ion in the MS spectra clearly showed the transformation from  $-\text{NH}_2$  in the phosphate group to  $-\text{OH}$  (Fig. 2).

Furthermore, a series of model peptides with a sequence similar to Ac-**S**WXNAKNG-CONH<sub>2</sub> where X = cysteine (**5**), aspartic acid (**7**), arginine (**8**), tyrosine (**9**), proline (**10**) or serine (**11**) were synthesized and investigated for the scope of this chemistry (ESI Fig. S6, S8–S12†). As outlined by the results in Table 1 (entries 7–11), the reactions from phosphopeptides **7–11** proceeded smoothly to afford the amidopyrophosphopeptide intermediates **23–27** with 93–96% and the corresponding pyrophosphopeptides **39–43** with 86–92% conversion over two steps (ESI Fig. S46–S55†). Despite the presence of other nucleophilic residues, the clean conversion indicated exclusive

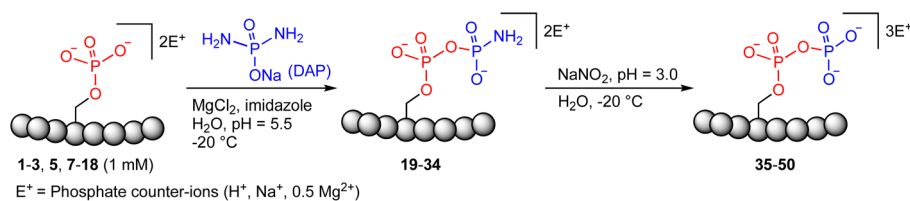
amidophosphorylation in the phosphoserine residue without any interferences from the existing tryptophan, lysine, histidine, aspartic acid, arginine, tyrosine, proline, or (non-phosphorylated) serine. In contrast, reactions of peptides lacking a phosphorylated serine gave no amidopyrophosphopeptide products (entries 4 and 6, and ESI Fig. S40 and S45†) even in the presence of a reactive hydroxyl and thiol group, respectively. It is noteworthy that no significant side reactions were observed during the nitrous acid-induced hydrolysis with a nucleophilic NH<sub>2</sub> group in lysine, tryptophan, histidine, or arginine residues, thus suggesting the high reactivity and chemoselectivity of the amino moiety in the amidophosphate group under our conditions.

Previous studies on peptide ligation<sup>39</sup> and isocyanate formation<sup>40</sup> showed that the optimal pH value for NaNO<sub>2</sub>-mediated oxidation of hydrazides was 3.0–4.0 where all amines from standard amino acid residues were protonated and thus rendered unreactive as nucleophiles. In our case, the amidopyrophosphate group remained active due to its low value of  $\text{pK}_a \approx 1.2$ <sup>25,26</sup> as well as the limited NaNO<sub>2</sub> added (equivalent amount to DAP), probably explaining the chemoselective HNO<sub>2</sub>-induced hydrolysis. In this context, the reaction of peptide **5** containing a cysteine is notable. As expected peptide **5** underwent, in the first step of amidophosphorylation, almost quantitative conversion (95%) to amidopyrophosphopeptide **22** (Table 1, entry 5, and ESI Fig. S41†). However, in the hydrolysis step with NaNO<sub>2</sub>, we observed the formation of the peptide nitrothioite (RSNO) as the major product – as indicated by the new peak in the LC-MS being +29 Da heavier than that of the free thiol peptide. It is known that the thiol group (RSH) could be oxidized using HNO<sub>2</sub> to generate nitrothioite (RSNO).<sup>41</sup> Nevertheless, the nitrothioite was cleanly reduced back to the original thiol by adding excess 4-mercaptophenylacetic acid (MPAA). By utilizing this protocol, the desired pyrophosphopeptide **38** with native cysteine was obtained with 66% conversion (ESI Fig. S42–S44†). Methionine, the other sulfur-containing residue, was reported to be stable with nitrous acid treatment,<sup>39</sup> and is, therefore, not expected to interfere in this protocol as well.

To expand the potential application of this methodology further, we subjected phosphothreonine- and phosphotyrosine-containing peptides (**12** and **13**, and ESI Fig. S13 and S14†) to the one-pot reaction conditions (Table 1, entries 12 and 13). Gratifyingly, both reactions furnished the expected pyrophosphopeptides **44** and **45** with 93% and 83% conversions *via* amidopyrophosphopeptides **28** and **29**, respectively (ESI Fig. S56–S59†). The reaction of phosphopeptide **14** (ESI Fig. S15†) containing multiple nucleophilic amino acid residues proceeded well to afford the expected pyrophosphopeptide **46** with 94% conversion (Table 1, entry 14, and ESI Fig. S60 and S61†). To demonstrate the practicality of the reactions, we scaled-up the reactions of **3**, **9**, **11** and **12** and the progress was monitored by LC-MS (ESI Fig. S62–S69†). All reactions proceeded to near complete conversion over the two steps to afford the desired pyrophosphopeptides, each of which were purified and isolated by preparative HPLC in 65%, 63%, 71% and 68% yields, respectively (Table 1, entries 3, 9, 11 and 12). The



Table 1 One-pot pyrophosphorylation of peptides using a sequential two-step protocol



Entry	Substrate peptide sequence <sup>a</sup>	Sequence origin	Amidopyrophosphorylated product <sup>c</sup> (% conversion)	Pyrophosphorylated product <sup>c</sup> (% conversion over two steps)
1	<b>1</b> Ac-WN <b>S</b> ANG-CONH <sub>2</sub>	Random	<b>19</b> (86)	<b>35</b> (85)
2	2 Ac-WKN <b>S</b> ANG-CONH <sub>2</sub>	Random	<b>20</b> (96)	<b>36</b> (95)
3	3 Ac- <b>S</b> WHNAANG-CONH <sub>2</sub>	Random	<b>21</b> (97)	<b>37</b> (96) (65) <sup>d</sup>
4	4 Ac-WN <b>S</b> ANG-CONH <sub>2</sub> <sup>b</sup>	Random	NR	NA <sup>f</sup>
5	5 Ac- <b>S</b> WCNAKNG-CONH <sub>2</sub>	Random	<b>22</b> (95)	<b>38</b> (66) <sup>g</sup>
6	6 Ac-W <b>C</b> NAKNG-CONH <sub>2</sub> <sup>b</sup>	Random	NR	NA <sup>f</sup>
7	7 Ac- <b>S</b> WDNAKNG-CONH <sub>2</sub>	Random	<b>23</b> (94)	<b>39</b> (92)
8	8 Ac- <b>S</b> WRNAKNG-CONH <sub>2</sub>	Random	<b>24</b> (93)	<b>40</b> (86)
9	9 Ac- <b>S</b> WYNAKNG-CONH <sub>2</sub>	Random	<b>25</b> (96)	<b>41</b> (90) (63) <sup>d</sup> (83) <sup>e</sup>
10	10 Ac- <b>S</b> WPNAKNG-CONH <sub>2</sub>	Random	<b>26</b> (94)	<b>42</b> (86)
11	11 Ac- <b>S</b> WSNAKNG-CONH <sub>2</sub>	Random	<b>27</b> (96)	<b>43</b> (90) (71) <sup>d</sup> (87) <sup>e</sup>
12	12 Ac- <b>T</b> WHNAANG-CONH <sub>2</sub>	Random	<b>28</b> (94)	<b>44</b> (93) (68) <sup>d</sup> (85) <sup>e</sup>
13	13 Ac- <b>Y</b> WHNAANG-CONH <sub>2</sub>	Random	<b>29</b> (90)	<b>45</b> (83)
14	14 Ac- <b>S</b> AGWSQKE-CONH <sub>2</sub>	Random	<b>30</b> (95)	<b>46</b> (94)
15	15 NH <sub>2</sub> -KE <b>S</b> DSSEDE-CO <sub>2</sub> H	RPA190 <sup>34</sup>	<b>31</b> (82)	<b>47</b> (79)
16	16 NH <sub>2</sub> -E <b>S</b> DLEKKRRE-CO <sub>2</sub> H	IC2C <sup>35</sup>	<b>32</b> (63)	<b>48</b> (60)
17	17 NH <sub>2</sub> -VNEDSP <b>S</b> SKL-CO <sub>2</sub> H	Gcr1 <sup>36,37</sup>	<b>33</b> (88)	<b>49</b> (86)
18	18 NH <sub>2</sub> -VQEP <b>T</b> EPDDL-CO <sub>2</sub> H	EIF2S2 <sup>37,38</sup>	<b>34</b> (70)	<b>50</b> (68)

<sup>a</sup> Amino acids highlighted in bold and red bear a phosphate group. Substrate numbers are given in bold. <sup>b</sup> Peptides that do not contain a phosphate group. <sup>c</sup> % conversions were estimated by reverse phase HPLC analysis based on the area-under-the-curve of the amidopyrophosphopeptide intermediates 19–34 and pyrophosphopeptides 35–50 vs. sum area of all peptidic-peaks. <sup>d</sup> The isolated yield (after two steps) of the purified pyrophosphopeptide by reverse phase HPLC purification. <sup>e</sup> The yield (after two steps) determined using standard curves of the purified pyrophosphopeptides. <sup>f</sup> NA = not applicable. <sup>g</sup> A nitrothioite peptide was observed by LC-MS as the product from oxidation of the thiol group by HNO<sub>2</sub>. Pyrophosphopeptide 38 (containing the thiol) was formed from reduction of the nitrothioite-intermediate by the addition of excess 4-mercaptophenylacetic acid (MPAA). Reaction conditions: (1) peptide (1 mM, 1.0 equiv.), DAP (5 mM, 5.0 equiv.), MgCl<sub>2</sub> (2 mM, 2.0 equiv.), imidazole (2 mM, 2.0 equiv.), H<sub>2</sub>O, pH = 5.5, –20 °C, 48–72 h; (2) NaNO<sub>2</sub> (5 mM, 5.0 equiv.), H<sub>2</sub>O, pH = 3.0, –20 °C, 20 h.

identities of the pyrophosphopeptide products were also established by <sup>31</sup>P-NMR (ESI Fig. S73–S78†). Four additional known sequences (15, 16, 17 and 18, and ESI Fig. S16–S19†) containing free N- and C-termini, derived from the DNA-directed RNA polymerase I subunit RPA190<sup>34</sup> (RPA190, Table 1, entry 15), the cytoplasmic dynein 1 intermediate chain 2<sup>35</sup> (IC2C, Table 1, entry 16), the glycolytic gene transcriptional activator<sup>36,37</sup> (Gcr1, Table 1, entry 17) and the mammalian protein eukaryotic translation initiation factor 2<sup>37,38</sup> (EIF2S2, Table 1, entry 18) were selected as substrates. The one-pot reactions of all these fully unprotected peptides 15, 16, 17 and 18 proceeded to give desired pyrophosphopeptides 47, 48, 49 and 50 with 79%, 60%, 86% and 68% conversion, respectively (ESI Fig. S79–S86†). The slight drop in yield for 16 and 18 may be a sequence effect and not due to the unprotected N- or C-terminus since the unprotected amino and carboxylic side chains (e.g., in sequences 2 and 7) have not impacted the yields. The reaction displayed excellent chemoselectivity considering the presence of multiple nucleophilic amino acids such as glutamic acid, aspartic acid, serine, and lysine in these peptides.

Tandem mass spectrometry (MS/MS) was reported to be used as a fragmentation technique for the identification of serine and threonine pyrophosphorylation.<sup>42</sup> To further confirm the constitutional integrity of the pyrophosphopeptide product, peptide 43 was characterized by collision-induced dissociation (CID) MS/MS spectrometry (Fig. 3). The observed fragment ion (M-178), generated from 43 by loss of the pyrophosphate motif, is a clear indicator for the pyrophosphorylated peptide and supports the assignment of phosphorylated serine as the site of pyrophosphorylation.<sup>42</sup> The b-ions and y-ions with varying lengths of amino acids retained by the amino and carboxyl-terminal part of M-178 were identified, precisely confirming the sequence of 43 as AcNH-pp**S**WSNAKNG-CONH<sub>2</sub> (ESI Fig. S87 and S88†). The MS/MS analysis revealed no modification of tryptophan, serine, or lysine side chains in 43. Combined with the exclusively single peak observed in HPLC for 43 (ESI Fig. S67†) and <sup>31</sup>P NMR (ESI Fig. S75†), this analysis again demonstrated the efficiency and chemoselectivity of the pyrophosphorylation reaction.

Next, we assessed the generality of the one-pot aqueous pyrophosphorylation strategy with a highly functionalized



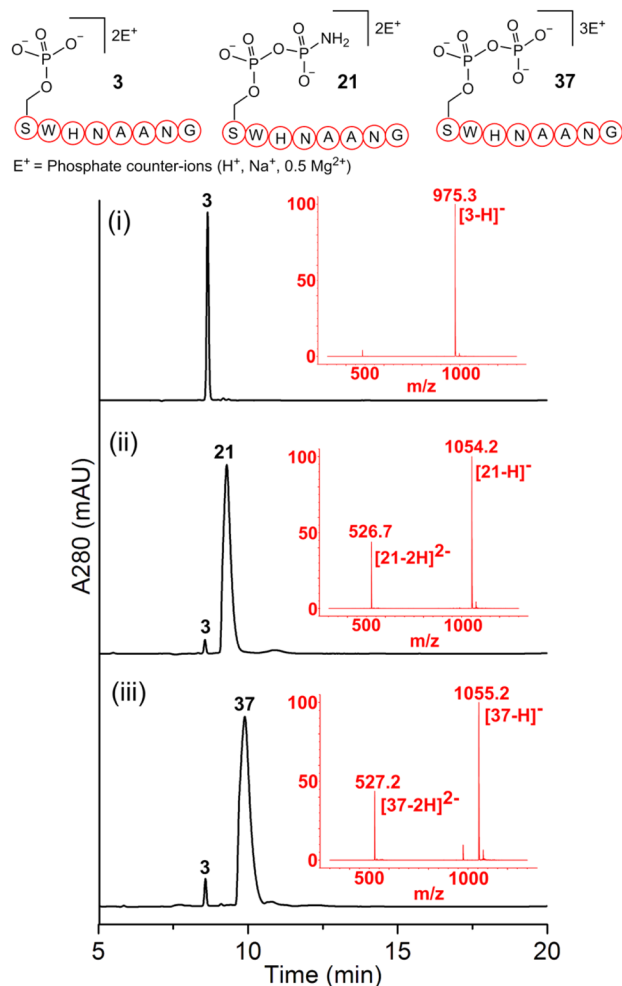


Fig. 2 Crude LC-MS chromatograms of reaction mixtures confirming the formation of pyrophosphorylated peptide 37 by a one-pot sequential amidophosphorylation-hydrolysis scenario. (i) The starting material 3 and the production of (ii) amidopyrophosphopeptide intermediate 21 and (iii) desired pyrophosphopeptide 37. The conversion in each step, as judged by using the HPLC traces, was nearly quantitative.

substrate, the Nopp140 peptide fragment containing amino acids 76–100, which is known to be pyrophosphorylated by inositol pyrophosphate *in vitro*.<sup>14</sup> The Nopp140 peptide fragment, a 25-residue peptide bearing a single phosphoserine, seven serines/threonines, five lysines, and eight glutamic/aspartic acids, seemed a challenging substrate to explore (Fig. 4a). The substrate 52 was synthesized by post-assembly phosphorylation and oxidation in the solid phase<sup>30,43</sup> in high efficiency and characterized by LC-MS (Fig. 4b, and ESI Fig. S1, S20 and S21†). Peptide 52 was reacted with DAP for 20 hours and was efficiently amidophosphorylated to form amidopyrophosphopeptide 53 in 75% conversion (Fig. 4a, and ESI Fig. S89†). Remarkably, subsequent treatment of 53 with  $\text{NaNO}_2$  in the same pot successfully afforded pyrophosphopeptide 54 with overall 70% conversion over two steps (Fig. 4a, and ESI Fig. S90†). The identities of 53 and 54 were confirmed by high-resolution mass spectrometry (HRMS) (Fig. 4c and d).

The efficient one-pot pyrophosphorylation of the highly functionalized 52 leading to the formation of 54 once again highlighted the high intrinsic nucleophilicity and selectivity of the phosphoserine residue towards DAP and the superior reactivity of the peptide-amidophosphate towards  $\text{HNO}_2$  even in a complex sequence. And yields of this one-pot strategy were much better than the previous results (*ca.* 11%) of the benzyl protected diphosphate derivative as reported in the literature.<sup>20</sup>

To further validate our methodology on producing valuable polyphosphorylated peptides, as a proof-of-principle experiment, we selected phosphoserine- and phosphothreonine-containing peptides (3 and 12, respectively) to generate triphosphopeptides *via* a one-pot sequential amidophosphorylation-hydrolysis scenario in water (Fig. 5). As observed previously, reactions of phosphopeptides 3 and 12 reached completion to quantitatively afford the pyrophosphopeptides 37 and 44 *via* amidopyrophosphopeptides 21 and 28, respectively (ESI Fig. S92, S93, S97 and S98†). By simply repeating the second amidophosphorylation and subsequent hydrolysis steps in the same pot, satisfactory conversions to final triphosphopeptides 56 and 58 were achieved in 61% and 70% yield, *via* amidotriphosphopeptides 55 and 57, respectively, as analysed by HPLC and anion exchange chromatography (ESI Fig. S94–S96 and S99–S101†). Successful triphosphorylation of phosphopeptides 3 and 12 could potentially broaden the applicability of this method in generating polyphosphorylated peptides.

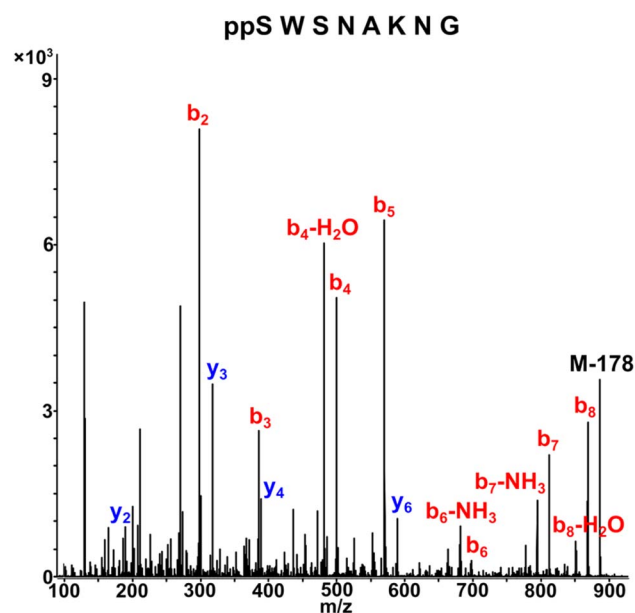


Fig. 3 CID MS/MS analysis of the pyrophosphopeptide 43 in positive ion mode, confirming the sequence as AcNH-ppSWSNAKNG-CONH<sub>2</sub>. The sequence was identified by matching b-ion (red) and y-ion (blue) fragments. M-178 was generated from 43 losing the pyrophosphate motif. The b-ions were retained by the amino-terminal part of M-178 and the y-ions were retained by the carboxyl-terminal part of M-178.



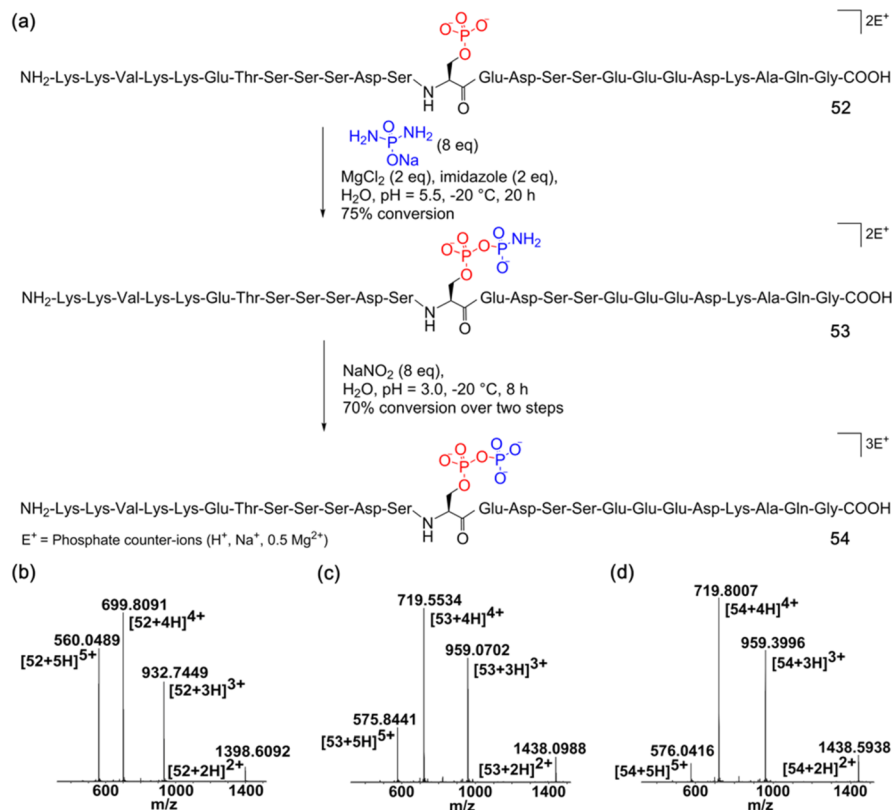


Fig. 4 Formation of the pyrophosphopeptide 54 from the highly functionalized Nopp140 peptide fragment. (a) General reaction scheme showing the pyrophosphorylation of the Nopp140 peptide fragment 52 to generate 54 via a one-pot sequential amidophosphorylation-hydrolysis scenario. (b)–(d) High resolution ESI-MS ( $m/z$ ) spectra in positive ion mode of the starting peptide 52, amidopyrophosphopeptide intermediate 53, and desired pyrophosphopeptide 54, respectively. Conversions were calculated by analytical HPLC based on the area-under-the-curve of 53 and 54 vs. sum area of all peptidic peaks.

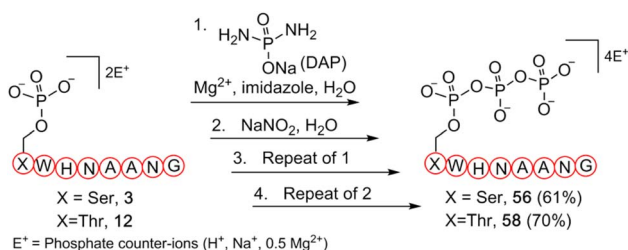


Fig. 5 Synthesis of triphosphopeptides 56 and 58 from respective phosphopeptides 3 and 12 via a one-pot four step sequential amidophosphorylation-hydrolysis scenario in water.

pyrophosphorylation of complex phosphopeptide targets. Furthermore, triphosphorylation of phosphopeptides was achieved by simply repeating the two steps of amidophosphorylation and hydrolysis in the same pot. Given the high yields and lack of byproducts, it is plausible that the thus-generated crude pyrophosphopeptides could be used directly in subsequent exploratory studies. For example, a repeat of this DAP-mediated phosphorylation has the potential to produce peptide- and protein-polyphosphates<sup>44,45</sup> in the same pot. Thus, we anticipate that this method will serve as a practical tool to quickly generate biologically relevant pyrophosphopeptides and explore their biochemistry in the emerging area of protein pyrophosphorylation.

## Conclusions

In summary, we have developed a one-pot strategy that enables efficient peptide pyrophosphorylation in water via a sequential amidophosphorylation-hydrolysis scenario. This method is operationally simple and highly chemoselective, obviating the need for orthogonal protecting groups for the canonical amino acid residues within the peptide. The efficacy of the pyrophosphorylation reaction was demonstrated by the broad scope of phosphopeptide substrates with different amino acid compositions. Notably, this method allowed the site-selective

## Data availability

The data supporting this article are available in the ESI.†

## Author contributions

H. Lin, L. J. Leman and R. Krishnamurthy conceived the project. H. Lin performed the experiments and analysed the data. H. Lin, L. J. Leman and R. Krishnamurthy wrote the manuscript and approved the final version.



## Conflicts of interest

There are no conflicts to declare.

## Acknowledgements

This work was supported by NSF and the NASA Astrobiology Program under the Centre for Chemical Evolution (CHE-150421) and a grant from the Simons Foundation to R. K. (327124FY19).

## References

- 1 Y. L. Deribe, T. Pawson and I. Dikic, *Nat. Struct. Mol. Biol.*, 2010, **17**, 666–672.
- 2 K. K. Biggar and S. S. Li, *Nat. Rev. Mol. Cell Biol.*, 2015, **16**, 5–17.
- 3 C. Choudhary and M. Mann, *Nat. Rev. Mol. Cell Biol.*, 2010, **11**, 427–439.
- 4 S. J. Humphrey, D. E. James and M. Mann, *Trends Endocrinol. Metab.*, 2015, **26**, 676–687.
- 5 K. W. Moremen, M. Tiemeyer and A. V. Nairn, *Nat. Rev. Mol. Cell Biol.*, 2012, **13**, 448–462.
- 6 E. Verdin and M. Ott, *Nat. Rev. Mol. Cell Biol.*, 2015, **16**, 258–264.
- 7 E. H. Fischer, D. J. Graves, E. R. S. Crittenden and E. G. Krebs, *J. Biol. Chem.*, 1959, **234**, 1698–1704.
- 8 T. Garcia-Garcia, S. Poncet, A. Derouiche, L. Shi, I. Mijakovic and M. F. Noirot-Gros, *Front. Microbiol.*, 2016, **7**, 184.
- 9 I. Kitazumi and M. Tsukahara, *FEBS J.*, 2011, **278**, 427–441.
- 10 D. V. Hoof, J. Munoz, S. R. Braam, M. W. H. Pinkse, R. Linding, A. J. R. Heck, C. L. Mummery and J. Krijgsveld, *Cell Stem Cell*, 2009, **5**, 214–226.
- 11 M. Mann, S. E. Ong, M. Gronborg, H. Steen, O. N. Jensen and A. Pandey, *Trends Biotechnol.*, 2002, **20**, 261–268.
- 12 A. Chakraborty, S. Kim and S. H. Snyder, *Sci. Signaling*, 2011, **4**, re1.
- 13 A. Saiardi, R. Bhandari, A. C. Resnick, A. M. Snowman and S. H. Snyder, *Science*, 2004, **306**, 2101–2105.
- 14 R. Bhandari, A. Saiardi, Y. Ahmadibeni, A. M. Snowman, A. C. Resnick, T. Z. Kristiansen, H. Molina, A. Pandey, J. K. Werner, K. R. Juluri, Y. Xu, G. D. Prestwich, K. Parang and S. H. Snyder, *Proc. Natl. Acad. Sci. U. S. A.*, 2007, **104**, 15305–15310.
- 15 A. Burton, C. Azevedo, C. Andreassi, A. Riccio and A. Saiardi, *Proc. Natl. Acad. Sci. U. S. A.*, 2013, **110**, 18970–18975.
- 16 A. Chakraborty, M. A. Koldobskiy, N. T. Bello, M. Maxwell, J. J. Potter, K. R. Juluri, D. Maag, S. Kim, A. S. Huang, M. J. Dailey, M. Saleh, A. M. Snowman, T. H. Moran, E. Mezey and S. H. Snyder, *Cell*, 2010, **143**, 897–910.
- 17 T. S. Lee, J. Y. Lee, J. W. Kyung, Y. Yang, S. J. Park, S. Lee, I. Pavlovic, B. Kong, Y. S. Jho, H. J. Jessen, D. H. Kweon, Y. K. Shin, S. H. Kim, T. Y. Yoon and S. Kim, *Proc. Natl. Acad. Sci. U. S. A.*, 2016, **113**, 8314–8319.
- 18 J. Worley, X. Luo and A. P. Capaldi, *Cell Rep.*, 2013, **3**, 1476–1482.
- 19 A. M. Marmelstein, J. A. M. Morgan, M. Penkert, D. T. Rogerson, J. W. Chin, E. Krause and D. Fiedler, *Chem. Sci.*, 2018, **9**, 5929–5936.
- 20 A. M. Marmelstein, L. M. Yates, J. H. Conway and D. Fiedler, *J. Am. Chem. Soc.*, 2014, **136**, 108–111.
- 21 T. Durr-Mayer, D. Qiu, V. B. Eisenbeis, N. Steck, M. Haner, A. Hofer, A. Mayer, J. S. Siegel, K. K. Baldrige and H. J. Jessen, *Nat. Commun.*, 2021, **12**, 5368.
- 22 T. M. Haas, S. Wiesler, T. Durr-Mayer, A. Ripp, P. Fouka, D. Qiu and H. J. Jessen, *Angew. Chem., Int. Ed.*, 2022, **61**, e202113231.
- 23 B. Roy, A. Depaix, C. Perigaud and S. Peyrottes, *Chem. Rev.*, 2016, **116**, 7854–7897.
- 24 S. M. Shepard, H. J. Jessen and C. C. Cummins, *J. Am. Chem. Soc.*, 2022, **144**, 7517–7530.
- 25 A. Osumah and R. Krishnamurthy, *ChemBioChem*, 2021, **22**, 3001–3009.
- 26 C. Gibard, S. Bhowmik, M. Karki, E. K. Kim and R. Krishnamurthy, *Nat. Chem.*, 2018, **10**, 212–217.
- 27 H. Lin, E. I. Jimenez, J. T. Arriola, U. F. Muller and R. Krishnamurthy, *Angew. Chem., Int. Ed.*, 2022, **61**, e202113625.
- 28 M. Ikehara, S. Uesugi and T. Fukui, *Chem. Pharm. Bull.*, 1967, **15**, 440–447.
- 29 W. P. Jencks and M. Gilchrist, *J. Am. Chem. Soc.*, 1964, **86**, 1410–1417.
- 30 T. J. Attard, N. O'Brien-Simpson and E. C. Reynolds, *Int. J. Pept. Res. Ther.*, 2007, **13**, 447–468.
- 31 E. Y. Song, E. I. Jimenez, H. Lin, K. L. Vay, R. Krishnamurthy and H. Mutschler, *Angew. Chem., Int. Ed.*, 2021, **60**, 2952–2957.
- 32 L. Y. An, Z. Dai, B. Di and L. L. Xu, *Molecules*, 2021, **26**, 750.
- 33 A. Kanavarioti, P. Monnard and D. W. Deamer, *Astrobiology*, 2001, **1**, 271–281.
- 34 S. G. Thota, C. P. Unnikannan, S. R. Thampatty, R. Manorama and R. Bhandari, *Biochem. J.*, 2015, **466**, 105–114.
- 35 M. Chanduri, A. Rai, A. B. Malla, M. Wu, D. Fiedler, R. Mallik and R. Bhandari, *Biochem. J.*, 2016, **473**, 3031–3047.
- 36 Z. Szijsyarto, A. Garedeu, C. Azevedo and A. Saiardi, *Science*, 2011, **334**, 802–805.
- 37 L. M. Yates and D. Fiedler, *ChemBioChem*, 2015, **16**, 415–423.
- 38 V. K. Pathak, P. J. Nielsen, H. Trachsel and J. W. B. Hershey, *Cell*, 1988, **54**, 633–639.
- 39 G. M. Fang, Y. M. Li, F. Shen, Y. C. Huang, J. B. Li, Y. Lin, H. K. Cui and L. Liu, *Angew. Chem., Int. Ed.*, 2011, **50**, 7645–7649.
- 40 A. A. Vinogradov, M. D. Simon and B. L. Pentelute, *Org. Lett.*, 2016, **18**, 1222–1225.
- 41 L. Grossi and P. C. Montevecchi, *J. Org. Chem.*, 2002, **67**, 8625–8630.
- 42 M. Penkert, L. M. Yates, M. Schumann, D. Perlman, D. Fiedler and E. Krause, *Anal. Chem.*, 2017, **89**, 3672–3680.
- 43 D. M. Andrews, J. Kitchin and P. W. Seale, *Int. J. Pept. Protein Res.*, 1991, **38**, 469–475.
- 44 C. Azevedo, T. Livermore and A. Saiardi, *Mol. Cell*, 2015, **58**, 71–82.
- 45 C. Azevedo, J. Singh, N. Steck, A. Hofer, F. A. Ruiz, T. Singh, H. J. Jessen and A. Saiardi, *ACS Chem. Biol.*, 2018, **13**, 1958–1963.

